



## Complexation of dichlorocarbene by methylanisoles

Robert A. Moss\*, Lei Wang, Christina M. Odorisio, Karsten Krogh-Jespersen\*

Department of Chemistry and Chemical Biology, Rutgers, The State University of New Jersey, New Brunswick, NJ 08903, United States

### ARTICLE INFO

#### Article history:

Received 16 December 2009

Revised 6 January 2010

Accepted 7 January 2010

Available online 14 January 2010

#### Keywords:

Carbenes

Kinetics

Spectroscopy

Calculations

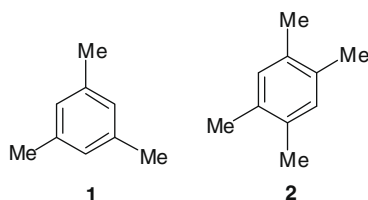
### ABSTRACT

Dichlorocarbene generated by laser flash photolysis of dichlorodiazirine readily forms UV–vis active  $\pi$ - and *O*-ylidic complexes with methylanisole derivatives.

© 2010 Elsevier Ltd. All rights reserved.

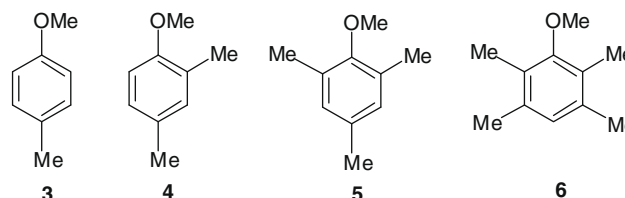
We recently reported that dichlorocarbene ( $\text{CCl}_2$ ), generated by laser flash photolysis (LFP) of dichlorodiazirine, formed  $\pi$ - and *O*-ylidic complexes with aryl ethers such as anisole, 1,3-dimethoxybenzene, and 1,3,5-trimethoxybenzene.<sup>1</sup> Detected by UV–vis spectroscopy, these complexes significantly retarded the addition of  $\text{CCl}_2$  to tetramethylethylene (TME). Structures, energetics, and spectral assignments for the complexes were provided by computational studies based on density functional theory.

Mesitylene (**1**) and durene (**2**) also retarded the addition of  $\text{CCl}_2$  to TME, by factors of 15 and 21, respectively, but we did not observe the UV absorptions computed for their  $\text{CCl}_2$  complexes in the 300–350 nm region.<sup>1</sup> The sensitivity of our LFP detection system may possibly be reduced in this spectral region due to strong background absorption by dichlorodiazirine ( $\lambda_{\text{max}}$  324, 359 nm in pentane).<sup>2</sup>



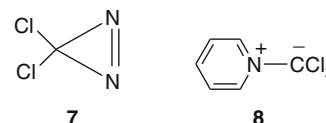
It occurred to us that the substitution of a methoxy group for a proton on arenes such as **1** or **2** would shift the electronic spectra of their  $\text{CCl}_2$  complexes toward the red, into the 400–500 nm region, where they might be more readily detected. For example, the UV–vis spectrum of the  $\text{CCl}_2$ /anisole complex features *O*-ylidic

and  $\pi$ -complex absorptions at 460 and 500 nm, respectively.<sup>1</sup> In the event, this proved a successful strategy, enabling us to describe here the  $\text{CCl}_2$  complexes of 4-methylanisole (**3**), 2,4-dimethylanisole (**4**), 2,4,6-trimethylanisole (**5**), and 2,3,5,6-tetramethylanisole (**6**).



Compounds **3** and **4** were commercially available, while trimethylanisole **5** was obtained by methylation of 2,4,6-trimethylphenol with dimethyl carbonate and a catalytic quantity of tetrabutylammonium iodide (93 °C, 19 h).<sup>3</sup> Tetramethylanisole **6** was similarly prepared from the corresponding phenol using 2,3,5,6-tetramethylphenol obtained by *ortho*-methylation of 2,3,5-trimethylphenol with ethyl(iodomethyl)zinc.<sup>4</sup> Compounds **5** and **6** were characterized by <sup>1</sup>H and <sup>13</sup>C NMR spectroscopy (see Figs. S-1–S-4 in the Supplementary data), and by mass spectrometry.

LFP of dichlorodiazirine (**7**)<sup>2</sup> in 1:1 (v/v) pentane solutions of methylanisoles **3–6** affords the UV–vis spectra shown in Figure 1. Each spectrum exhibits two distinct absorption peaks in the 450–550 nm region, which we attribute to  $\text{CCl}_2$  complexes.



\* Corresponding authors. Tel.: +1 732 445 2606; fax: +1 732 445 5312 (R.A.M.).  
E-mail addresses: [moss@rutchem.rutgers.edu](mailto:moss@rutchem.rutgers.edu) (R.A. Moss), [krogh@rutchem.rutgers.edu](mailto:krogh@rutchem.rutgers.edu) (K. Krogh-Jespersen).

Table 1 records the wavelengths of these species, and includes the previously reported *O*-ylidic and  $\pi$ -complexes of the parent anisole.<sup>1</sup>

We note that both absorptions, in each spectrum of Figure 1, shift to longer wavelengths in response to each additional methyl substituent imposed on the parent anisole structure.  $\text{CCl}_2$  usually<sup>5</sup> (although not always<sup>6</sup>) behaves as an electrophile, so that this observation accords with enhanced electron donation by the methylanisole derivative to an electrophilic  $\text{CCl}_2$ , buttressed by the successive methyl group substitutions.

Theoretical considerations generally support this view: calculations based on density functional theory (see the Supplementary data for details) provide structures and energetics for the transient  $\text{CCl}_2$ /methylanisole species and largely rationalize their absorption spectra. Computed complexation enthalpies are low for all identified complexes, spanning a range from  $-2.6$  to  $-4.3$  kcal/mol, whereas the (standard) free energies are well into the positive realm ( $\sim 4$ – $5$  kcal/mol, PBE/6-311+G(d); see Table S-1 in the Supplementary data). Thus, the binding of individual complexes is weak. However, there are many  $\text{CCl}_2$ /methylanisole configurations with slightly variant carbene-ligand orientations and/or interaction distances, all of approximately equal energies, and so the net number of complexes formed is sufficiently large to be detected.

The binding enthalpies tend to become more favorable as the degree of methylation increases, in particular for the  $\pi$ -type complexes, whereas the binding enthalpies of the *O*-ylidic complexes lie within a smaller range of  $-2.6$  to  $-3.5$  kcal/mol. Generally, binding increases with increasing electron richness of the aromatic ring, but we find no simple relationship between net atomic charge

**Table 1**

Absorption maxima of  $\text{CCl}_2$ -methylanisole complexes<sup>a</sup>

Ligand	$\lambda_{\text{max}}$ (nm)	
Anisole <sup>b</sup>	460	500
<b>3</b>	484	516
<b>4</b>	488	520
<b>5</b>	508	532
<b>6</b>	516	548

<sup>a</sup> In 1:1 (v/v) pentane/ligand solutions.

<sup>b</sup> From Ref. 1.

(C or O) at a particular methylanisole binding site and binding enthalpy. (See Fig. S-9 in the Supplementary data for net atomic charges of the methyanisoles.)

Illustrative examples of typical *O*-ylidic and  $\pi$ -complexes are shown in Figure 2, using 2,4-dimethylanisole as the representative ligand. In the *O*-ylidic complexes (Fig. 2, left-hand structure), the C(carbene)-O distance is in the 2.4–2.6 Å range, and the O atom rehybridizes toward tetrahedral coordination. The smallest C(carbene)-C(phenyl) interaction distances in the  $\pi$ -complexes (Fig. 2, center) are slightly longer at 2.6–2.9 Å; C(carbene) is always located vertically above a C(phenyl) atom, and one of the Cl atoms points toward the center of the phenyl ring.

The electronic transitions of lowest energy computed for each complex (TD-B3LYP/6-311+G(d)//PBE/6-311+G(d)) are also listed in Table S-1. As detailed previously,<sup>1</sup> the *O*-ylidic species was computed to be the thermodynamically most stable of the parent  $\text{CCl}_2$ /anisole complexes ( $\Delta G = 3.7$  kcal/mol), while the relative stabilities

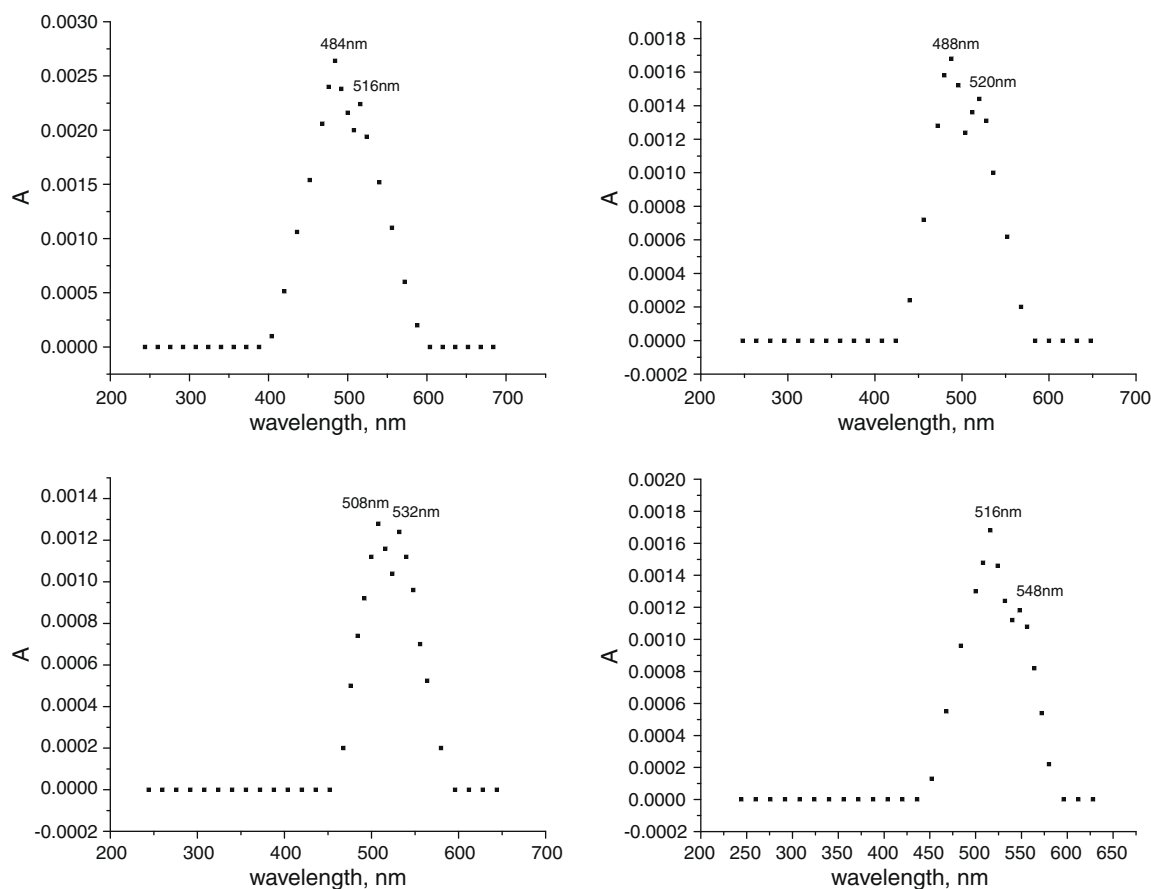


**Figure 1.** Complexes of  $\text{CCl}_2$  with (upper left) 4-methylanisole (**3**); (upper right) 2,4-dimethylanisole (**4**); (lower left) 2,4,6-trimethylanisole (**5**); (lower right) 2,3,5,6-tetramethylanisole (**6**). All spectra were determined in 1:1 (v/v) pentane-ligand solutions, under nitrogen, 150 ns after the laser flash. The axes of each graph are labeled 'A' (for absorbance) and 'wavelength, (nm)'.<sup>1</sup>

of the three different  $\pi$ -complexes were about equal ( $\Delta G \sim 4.4$ – $5.0$  kcal/mol). The experimental absorption around 460 nm for  $\text{CCl}_2$ /anisole was assigned to the *O*-ylidic complex for which a strong absorption band with significant  $\text{O} \rightarrow \text{p}(\text{CCl}_2)$  character was predicted at 486 nm ( $f = \text{oscillator strength} = 0.11$ ). The absorption observed at 500 nm was assigned to the  $\pi$ -complexes collectively; individual absorbances [ $\pi(\text{anisole}) \rightarrow \text{p}(\text{CCl}_2)$ ] were predicted at 513 nm ( $f \sim 0.1$ ) for both the C2 and C4 coordinated complexes and at 534 nm ( $f = 0.08$ ) for C6 coordination.<sup>1</sup>

In the present study, the absorptions of the  $\text{CCl}_2$ /4-methylanisole complexes are red-shifted by about 20 nm relative to the anisole complexes. The *O*-ylidic  $\text{CCl}_2$ /3 complex is computed to be the most stable and to absorb at 507 nm ( $f = 0.14$ ), so that we assign this species as responsible for the observed absorption at 484 nm (see Fig. 1). We have located  $\pi$ -complexes at every possible phenyl ring location (Table S-1), and sites C5 and C6 are particularly favorable for  $\text{CCl}_2$  binding. The resulting complexes absorb at 544 nm ( $f = 0.09$ , C5) and 557 nm ( $f = 0.08$ , C6), respectively, consequently, we assign these complexes as the dominant contributors to the absorption observed at 516 nm (Fig. 1).

For  $\text{CCl}_2$  and 2,4-dimethylanisole (4), the calculations find the  $\pi$ -complexes at the C1 and C6 binding sites to be the most stable (cf., Fig. 2, center); both sets of complexes are predicted to absorb around 570 nm with substantial intensities ( $f \sim 0.1$ ), and we assign these complexes to the experimental absorption peak at 520 nm in Figure 1. The *O*-ylidic complex (Fig. 2, left) and  $\pi$ -complexes formed at C5 absorb about 30–35 nm further to the blue in the 535–540 nm region (both absorptions have  $f = 0.12$ ), and we assign these complexes to the observed absorption peak at 488 nm in Figure 1.

In ligands 5 and 6, the methyl group of the methoxy unit rotates to assume a position perpendicular to the aryl ring plane because of steric hindrance from the adjacent methyl groups on C2 and C6, thus diminishing  $\pi$ -donation by the methoxy group. Although the orbital energies of the upper occupied  $\pi$ -orbitals of the arene become less negative (i.e., are destabilized) from anisole to the methylanisoles 3 and 4, the rotation of the methoxy group leads to a reversal of this trend for the HOMO's of 5 and 6 (Table S-2 in the Supplementary data). The energy of the donor orbital enters directly into the expression for the electronic transition energy and, as a result, the  $\text{CCl}_2$  complexes of 5 and 6 are computed to experience blue shifts relative to analogous complexes formed with 3 and 4. In contrast, the observed absorptions for the  $\text{CCl}_2$  complexes of 5 and 6 are red shifted by 10–30 nm, relative to complexes with 4 (cf. the spectra in Fig. 1 and the data in Table 1). For  $\text{CCl}_2$  and 5 we located complexes of equal stability ( $\Delta G \sim 3.8$  kcal/mol) at C1 and C3 (the C1 complex is shown in Fig. 2, right) which should absorb at 490 nm and 511 nm, respectively, with  $f \sim 0.1$ . The *O*-ylidic complex is computed to be slightly less stable ( $\Delta G \sim 4.4$  kcal/mol) and absorb slightly further to the blue at

**Table 2**Rate constants for the addition of  $\text{CCl}_2$  to TME<sup>a</sup>

Solvent or additive	$k_{\text{add}}$ ( $\text{M}^{-1} \text{s}^{-1}$ )	$k_{\text{pent}}/k_{\text{add}}$
Pentane <sup>b</sup>	$4.7 \times 10^9$	1.0
Anisole <sup>c</sup>	$2.6 \times 10^8$	18
3	$1.0 \times 10^8$	47
4	$7.8 \times 10^7$	60
5	$5.5 \times 10^7$	85
6	$4.9 \times 10^7$	96

<sup>a</sup> At 25 °C; [pyridine] = 0.12 mM for anisole, 3, and 4; 2.4 mM for 5 and 6.<sup>b</sup> Rate constant from Ref. 8.<sup>c</sup> Rate constant from Ref. 1.

464 nm ( $f \sim 0.1$ ). Similarly, for  $\text{CCl}_2$  and 6, we compute  $\pi$ -complexes at C1 and C4 which absorb at 506 nm and 486 nm, respectively, with  $f \sim 0.1$ . Two absorptions of the *O*-ylidic complex should center around 455 nm with overall intensities similar to those of the  $\pi$ -complexes.

In summary, for  $\text{CCl}_2$  complexes with methylanisoles 5 and 6, the calculations predict three absorption peaks in the 460–510 nm region of similar intensities and nearly equidistant spacing ( $\sim 20$  nm), whereas experiment shows only two distinct peaks in the 510–550 nm region (cf., Fig. 1 and Table 1). We are thus unable to make specific assignments of the  $\text{CCl}_2$ /5 or  $\text{CCl}_2$ /6 absorption spectra to individual complexes.

In keeping with previous observations,<sup>1</sup> complexation of  $\text{CCl}_2$  with methylanisoles 3–6 diminishes the rate constants for the addition of  $\text{CCl}_2$  to TME. We used the pyridine ylide method<sup>1,7</sup> to determine rate constants for the addition of  $\text{CCl}_2$  to TME in pentane and in the presence of anisole and the methylanisoles; cf. Table 2.

The apparent rate of the formation of the  $\text{CCl}_2$ -pyridinium ylide 8, measured at 404 nm in pentane or a pentane-additive solution, increased upon the addition of TME at a constant concentration of pyridine. A correlation of the observed rate constants for the formation of 8 versus [TME] was linear and its slope gave  $k_{\text{add}}$  for the addition of  $\text{CCl}_2$  to TME.<sup>7a</sup> In this way, we determined that  $\text{CCl}_2$  generated by LFP of diazirine 7 adds to TME in pentane with  $k_{\text{add}} = 4.7 \times 10^9 \text{ M}^{-1} \text{ s}^{-1}$ .<sup>8</sup> Repetition of this experiment in 1:1 anisole-pentane gave  $k_{\text{add}} = 2.6 \times 10^8 \text{ M}^{-1} \text{ s}^{-1}$ ; see Figure 8 of Ref. 1 and Table 2, above.

Similarly, we measured  $k_{\text{add}}$  for the  $\text{CCl}_2$ -TME addition in 1:1 solutions of pentane and methylanisoles 3–6. The results appear in Table 2, and the corresponding correlations of  $k_{\text{obs}}$  with [TME] are shown in Figs. S-5–S-8 of the Supplementary data. Table 2 reveals that successive methylations of anisole lead to increased retardation of  $\text{CCl}_2$  addition to TME. One interpretation holds that  $\text{CCl}_2$  complexes with increasingly methylated anisole derivatives are not only more stable, but also slower to transfer their complexed carbene to TME, possibly due to a combination of steric and stabilization effects. Alternatively, if complexation is reversible, the more

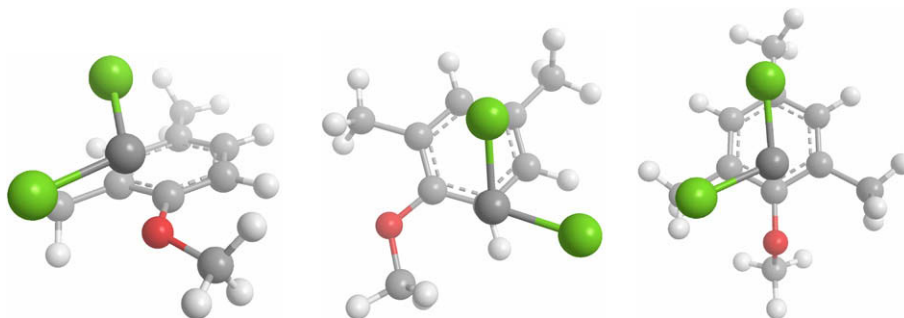


**Figure 2.** Perspective and depth-fading illustration of  $\text{CCl}_2$ /methylanisole complexes: *O*-ylidic  $\text{CCl}_2$ /2,4-dimethylanisole complex (left);  $\text{CCl}_2$ /2,4-dimethylanisole  $\pi$ -complex at C6 (center);  $\text{CCl}_2$ /2,4,6-trimethylanisole  $\pi$ -complex at C1 (right).

highly methylated anisoles may sequester more  $\text{CCl}_2$  at equilibrium, thus leaving less free  $\text{CCl}_2$  available for addition to TME.

Tri- and tetramethylanisoles **5** and **6** are more potent than their non-methoxy analogs, mesitylene (**1**) and durene (**2**), at retarding  $\text{CCl}_2$  addition to TME: the ratios of  $k_{\text{add}}$  for **1** versus **5** and **2** versus **6** are 5.8 and 3.1, respectively.<sup>9</sup> These disparities probably reflect the additional stabilization conferred upon the mesitylene or durene  $\text{CCl}_2$  complexes by substitution of the electron-donating methoxy group which converts them to complexes of **5** and **6**, respectively.

In conclusion,  $\text{CCl}_2$  generated by LFP of dichlorodiazirine forms readily visualized  $\pi$ - and *O*-ylidic complexes with methylanisoles **3–6**. These complexes are UV–vis active and are substantiated by DFT computations. Complexation of  $\text{CCl}_2$  by the methylanisoles retards the addition of the carbene to TME by factors of about 50–100.

#### Acknowledgments

We are grateful to the National Science Foundation and to the Petroleum Research Fund for financial support.

#### Supplementary data

Supplementary data associated with this article can be found, in the online version, at doi:10.1016/j.tetlet.2010.01.023.

#### References and notes

1. Moss, R. A.; Wang, L.; Odorisio, C. M.; Zhang, M.; Krogh-Jespersen, K. *J. Phys. Chem. A* **2010**, *114*, 209.
2. Moss, R. A.; Tian, J.; Sauers, R. R.; Ess, D. H.; Houk, K. N.; Krogh-Jespersen, K. *J. Am. Chem. Soc.* **2007**, *129*, 5167.
3. Taniguchi, Y.; Nobori, T.; Yamamoto, Y. *Jpn. Kokai Tokkyo Koho Japanese Patent 2004 123541* (22 April 2004). We thank Professor Akira Sekiguchi for a translation of the procedure.
4. Lehnert, E. K.; Sawyer, J. S.; McDonald, T. L. *Tetrahedron Lett.* **1989**, *30*, 5215.
5. Moss, R. A. *Acc. Chem. Res.* **1980**, *13*, 58.
6. Moss, R. A.; Zhang, M.; Krogh-Jespersen, K. *Org. Lett.* **2009**, *11*, 1947.
7. (a) Jackson, J. E.; Soundararajan, N.; Platz, M. S.; Liu, M. T. H. *J. Am. Chem. Soc.* **1988**, *110*, 5595; (b) Presolski, S. I.; Zorba, A.; Thamattoor, D. M.; Tippmann, E. M.; Platz, M. S. *Tetrahedron Lett.* **2004**, *45*, 485.
8. Moss, R. A.; Tian, J.; Sauers, R. R.; Skalit, C.; Krogh-Jespersen, K. *Org. Lett.* **2007**, *9*, 4053.
9. Values of  $k_{\text{add}}$  for **1** ( $3.3 \times 10^8 \text{ M}^{-1} \text{ s}^{-1}$ ) and **2** ( $1.5 \times 10^8 \text{ M}^{-1} \text{ s}^{-1}$ ) appear in Ref. 1.